

UNCLASSIFIED

Defense Technical Information Center
Compilation Part Notice

ADP011915

TITLE: Photoinduced Optical Effects in BiB3O6 Glass

DISTRIBUTION: Approved for public release, distribution unlimited

This paper is part of the following report:

TITLE: International Conference on Solid State Crystals 2000: Growth, Characterization, and Applications of Single Crystals Held in Zakopane, Poland on 9-12 October 2000

To order the complete compilation report, use: ADA399287

The component part is provided here to allow users access to individually authored sections of proceedings, annals, symposia, etc. However, the component should be considered within the context of the overall compilation report and not as a stand-alone technical report.

The following component part numbers comprise the compilation report:

ADP011865 thru ADP011937

UNCLASSIFIED

Photoinduced optical effects in BiB₃O₆ glass

I. V. Kityk^a, M. Makowska-Janusik^a, A. Majchrowski^b

^aSolid State Department WSP, 42 217 Częstochowa, Al. Armii Krajowej 13/15, Poland

^bInstitute of Applied Physics MUT, 00-908 Warsaw, ul. Kaliskiego 2, Poland

ABSTRACT

A new borate material, BiB₃O₆ (BiBO), has been reported to have extremely high nonlinear optical (NLO) coefficient. In our investigations we obtained both glass and single crystals of BiBO. Owing to its composition, the material is very viscous when molten. This factor causes serious problems both during synthesis and crystallization of BiBO. In this paper only properties of BiBO glass are reported. We found that for the increase of the long-range ordering the photoinduced optical second harmonic generation (SHG) shows a maximum, which is shifted towards the lower photoinducing power with the increase of the temperature. Maximal value of SHG was about 0.081 pm/V at 1.06 μ m radiation from YAG:Nd laser (W=30MW, τ =35ps).

keywords: borate glass, bismuth borate, nonlinear optical properties.

1. INTRODUCTION

In recent years borates have been intensively investigated due to their excellent nonlinear optical and laser properties. Among the newly synthesized borate single crystals, it is necessary to point out the following: BiBO,¹ YCOB,² KAB,³ and CLBO.⁴ Crystalline BiBO was reported by Liebertz et al.¹ to have extremely high NLO coefficient for SHG of 3.2 pm/V. This value is larger than that of widely used NLO crystals such as β -BaB₂O₄ (BBO)⁵ or KTiOPO₄ (KTP).⁶

In our investigations both BiBO crystals and glass were produced. In this paper we report only on photoinduced optical effects in BiBO glass, the NLO properties of BiBO single crystals will be published elsewhere. Molten borates are characterized by very large viscosity and its steep temperature dependence.⁷ Some molten borates have viscosity approaching 10³ poise near their temperature of crystallization. The segregation of melt constituents on the melt-crystal interface is very slow and even the slightest changes of the melt temperature can deteriorate the growth conditions, what in consequence gives crystals with poor quality. Additionally such melts show strong tendency to glass formation, so it is very difficult to initiate their crystallization. On the other hand this property of molten borates makes obtaining them in form of glass relatively easy. Decreasing the temperature of molten borates below the melting point causes rapid increase of melt viscosity, what reduces the atomic mobility in the melt. The nucleation of crystallization centres in such melts is very slow and as a consequence glass formation is observed.

The starting material was synthesized from stoichiometric amounts of B₂O₃ and Bi₂O₃ in a platinum crucible. To obtain material with known composition boron oxide was molten first to remove water which is easily absorbed by this compound. In next step, after finding the mass of molten B₂O₃ appropriate amount of Bi₂O₃ was added to the crucible. Owing to high viscosity of molten BiBO it was very difficult to obtain homogeneous melt which had to be stirred with the use of a platinum mixer at 850°C. The process lasted several days until the melt became totally transparent. BiBO glass was produced by rapid cooling of the melt to temperatures below 600°C, then rods of different diameters were formed from the viscous melt.

For investigations we have chosen the specimens with different degree of crystallinity. The degree of crystallinity was evaluated as a ratio of intensity of the first crystalline maximum to the total amorphous-like background. The corresponding parameter was introduced by direct ratio of the first X-ray maximum to the total amorphous-like background.

2. MEASUREMENT PROCEDURE

The output optical SHG light intensities were detected using FEU-79 (FEU-39) photomultipliers. The measurements were carried out in the single-pulse regime, with a pulse frequency repetition of 12 Hz with the tunable pulse duration within 1.0 ps. From expression $T \approx 1 - \beta I I_p$, where β is the two-photon absorption (TPA) coefficient, l is the thickness of specimen (about 0.5 mm), T - intensity dependent transparency, we have determined the TPA coefficient. The nonlinear TPA was extracted from the intensity-dependent transparency measurements. Simultaneously we have subtracted an influence of linear absorption (220 cm⁻¹, λ =530 nm) and of Fresnel reflection 0.04. The averaging statistics over the sample surface was performed in order to average a space nonuniformity in the optical constant distribution.

During the evaluations of time delayed nonlinear optical response we performed measurements of the light intensities at ω and 2ω laser frequencies with the time step of about 0.06 ps. This was ensured using the electronic boxcar (GENETIC12 M) used in the time-synchronized pump-robe conditions. The calculations of the nonlinear optical susceptibility were done from the expression:

$$I(2\omega, t) = \frac{2\mu_0^{3/2} \varepsilon_0^{3/2} \omega^2 \chi_{ijk}^2 I(\omega, t - \tau)^2 d^2 \left[\frac{\sin(d\Delta k(t)/2)}{d\Delta k(t)/2} \right]^2}{\pi R_0^2 n(2\omega)n(\omega)^2} \quad (1)$$

Here R_0 is a radius of the pumping beam which possesses gaussian-like form; $n(2\omega)$ and $n(\omega)$ – refractive indices for the pumping and PISHG doubled frequencies during the photo-pumping; χ_{ijk} – components of the second order nonlinear optical susceptibility determined for different angles of incident light.

To exclude an influence of the hyper-Raman scattering, we have performed the additional investigations of the scattered light up to 3000 cm^{-1} , starting from the wavelength light of 530 nm. Three hyper-Raman maxima between 1200 cm^{-1} and 1800 cm^{-1} were observed with the intensities at least 13 times weaker than the probing phototransparent signal. In the case of the Raman and hyper-Raman measurements we have used argon laser at 522 nm Ar^+ laser line and Spex Triplemate spectrometer. A position-sensitive photomultiplier calibrated using helium-neon gaseous mixture discharge was used to detect the scattered light quanta.

Photoinduced changes of the investigated specimens were done by light of the Q-switched Ti-sapphire laser. The pulses of this laser were multiplied by frequency and their power was varied within the 0.1 – 12 MW, the corresponding pulse duration was changed within the 2- 65 ps. As a probing second harmonic generation source the pulses of the YAG-Nd laser with wavelength $1.06 \mu\text{m}$ and pulse duration 2 ps were used. The output second harmonic generation ($\lambda=0.53 \mu\text{m}$) and pumping ($\lambda=1.06 \mu\text{m}$) signals were spectrally separated by grating monochromator SPM-3. The detection of the corresponding signals was performed by 450 ps boxcar connected with the PDP computer.

From the Fig. 1 one can clearly see that increasing photoinducing power E and disordering (otherwise connected with degree of crystallinity dc) stimulate the enhanced value of the SHG. This indicates an additional enhancement of the output SHG signal due to the disordered non-centrosymmetric voids.

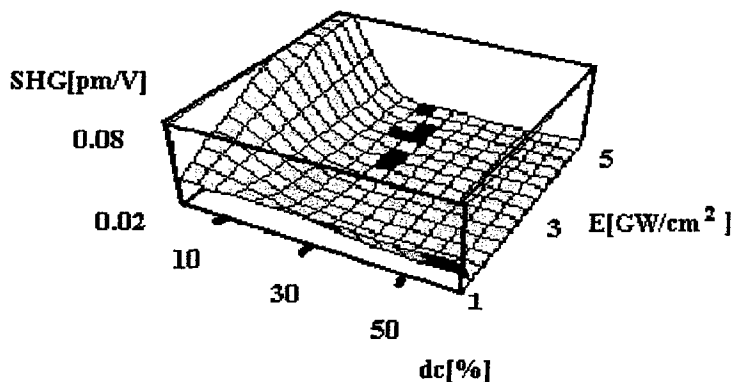


Fig. 1. Dependence of the SHG versus the photoinducing power E and degree of crystallinity dc .

Special interest causes influence of scalar hydrostatic pressure effectively varying the inter-atomic bonds. From Fig. 2 one can see that increasing hydrostatic pressure suppresses the output TPA signal. At the same time the decreasing temperature favours increasing TPA. These values are described by the fourth rank tensors and in this case dominant contribution gives randomly oriented vacancies. This fact is very important for possibility of operation by the output TPA in the partially disordered materials due to varying dc .

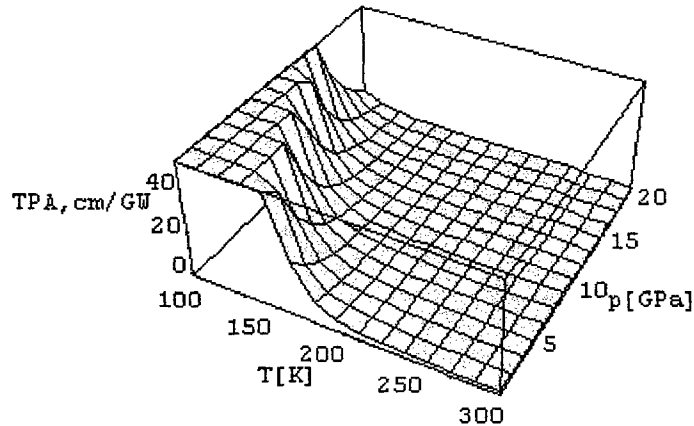


Fig. 2. Temperature dependence of the TPA versus the hydrostatic pressure and temperature. All the measurements were done for the $dc = 12\%$.

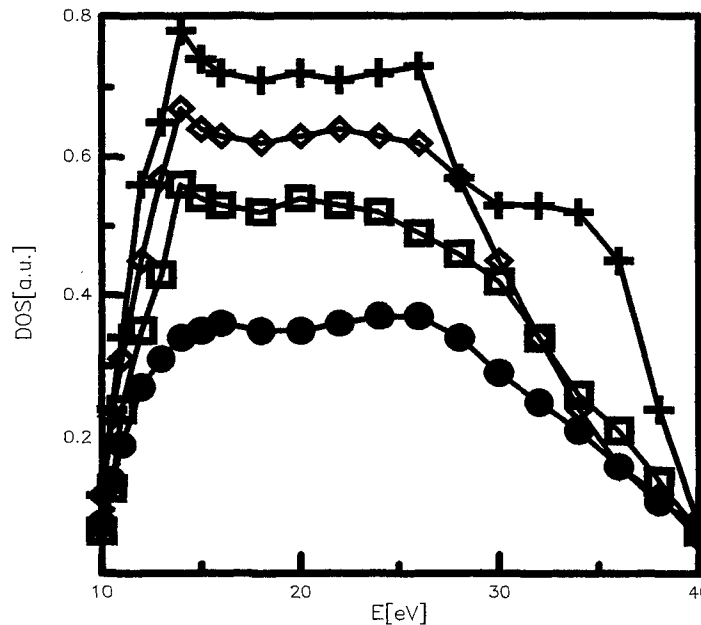


Fig. 3. Dependence of the density of states of BiBO glass on energy for the different degree of crystallinity: \bullet - 5%; \square - 12%; \diamond - 24%; $+$ - 38%.

From Fig. 3 one can see additional redistribution of the density of states for the amorphous-like glasses of different ordering obtained from X-ray photoelectron spectroscopy. One can clearly see that enhanced disorder substantially decreases total density of states. In order to explain the observed phenomena we have done theoretical simulations using the molecular dynamics simulation and solid state calculations. Generally the method is similar to the described in the Ref. 8.

Calculations of the band electronic structure have been performed taking into account electron-phonon interactions. The calculations have been carried out using *ab initio* norm-conserving pseudopotential method within a Local Density Approximation (LDA). The degree of crystallinity has been taken into account using an extended quasi-Brillouin zone. We have separated contribution of the electron and phonon subsystems, effectively contributing to the nonlinear optical susceptibilities. The phonon modes (within the BiBO glasses) have been calculated using a harmonic approximation, i.e.:

$$d^2\Psi_k/dQ_k^2 + [4\pi^2 \mu_k h^{-2} \Omega_k^2] \Psi_k = 0 \quad (2)$$

where Ψ_k is a phonon-like wave function corresponding to k -th normal coordinate Q_k within the BiBO crystallites, renormalized by surrounding long-range amorphous-like background; μ_k denotes a reduced mass of ions in the k -th phonon mode. Second derivatives of the effective crystalline potential (renormalized by surrounding amorphous-like background) play a dominant role in the observed phonon modes.

An eigen-energy of the k -th phonon mode can be written in the following standard form:

$$\Omega_k(v_k) = 2\Omega_{k0}(v_k + 1/2) \quad (3)$$

where $\Omega_{k0} = h/(f_k/\mu_k)^{1/2}/2$ is an eigen-energy for the zero-point quasi-phonons and $v_k = 0, 1, 2, \dots$ are phonon quantum numbers associated with the following wave functions:

$$\Psi_k(Q_k) = (2\Omega_{k0}/\pi)^{1/4} (2^{v_k}/v_k!)^{-1/2} \exp(-\Omega_{k0} Q_k) H_{v_k}((2\Omega_{k0})^{1/2} Q_k) \quad (4)$$

where $H_{v_k}(x)$ is a Hermite polynomial.

In order to model the vacancy-induced changes, it should be noticed that the electron-phonon interactions should be considered, particularly for the low-frequency phonon modes that could be in a frequency resonance with vacancy resonances. Calculations of the electron-phonon anharmonic potential have been carried out (this can be seen in absorption spectra) in a nonlinear approximation, i.e.:

$$V_{e-ph}(r_i) = e^2 \sum_{ms} M_{ms}^{-1/2} [Z_{ms}(r_s - u_{ms}) |r_s - u_{ms}|^{-3} - \sum_{m's'} Z_{m's'}(r_s - u_{m's'}) |r_s - u_{m's'}|^{-3}] \quad (5)$$

where M_{ms} and eZ_{ms} is effective ionic mass and charge for corresponding ions numbered by m and s , respectively. The intra- as well as inter-crystalline interactions have been taken into account. Moreover, two effective wavevectors have been introduced. The first one, traditionally corresponding to the ordered crystallite units and the second one, quasi-wavevector that is built on the effective molecular sphere originating from the amorphous-like disorder. Influence of the interface region (between the effective BiBO nanocrystallites and the glass-like background) has been extracted by performing a derivative procedure that eliminates possible potential jumps on the crystallite borders. The $u_{ms,m's'}$ vector is a relative displacement of two ions from their equilibrium positions r_s and $r_{s'}$. A probability of a one-phonon transition induced by the phonon of a frequency Ω_k is equal to:

$$\Xi(\Omega_k) = 4(h/2\pi)^{-2} c^3 H^{-1} g^{-1}(r_i) (E_{el} - \Omega_k)^2 \Theta(\Omega_k) \quad (6)$$

where H is a sum of the η and ξ level widths, E_{el} is an electron transition energy, Ω_k denotes a phonon energy and $g(r_i)$ is a degeneration degree of the corresponding electron energy levels. The parameter $\Theta(\Omega_k)$ is equal to:

$$\Theta(\Omega_k) = \sum_{\eta} g(\eta) \sum_{\xi} g(\xi) \left\{ \left| \sum_{\varphi} \langle \eta, \eta_{\Omega} | V_{e-ph}(\mathbf{r}_i) | \varphi, \eta_{\Omega+1} \rangle \langle \varphi | \mathbf{d} | \xi \rangle (E_{\xi} - E_{\eta} + \Omega_k)^{-1} + \sum_{\varphi} \langle \eta | \mathbf{d} | \varphi \rangle \langle \varphi, \eta_{\Omega} | V_{e-ph}(\mathbf{r}_i) | \xi, \eta_{\Omega-1} \rangle (E_{\xi} - E_{\eta} - \Omega_k)^{-1} \right\}^2 \theta \quad (7)$$

here η and ξ are lower and upper electron energy levels, respectively; φ denotes a virtual electron state, \mathbf{d} is an electric dipole moment for a given spectral transition. The summation is performed over all degenerated initial and final states. Orthogonalization to the highly delocalized states has been carried out by the orthogonalisation procedure of the Legendre polynomials. The symbol θ denotes averaging over all occupied phonon states for phonons with frequency Ω_k . The symmetric phonon modes included in the electron-phonon interaction (see Eq. 5) are renormalized by the normal coordinates that leads to:

$$\Theta(\Omega_k) = C_{\eta\xi}^{\gamma}(r_{\lambda}^{\Delta}) C_{\eta\xi}^{\gamma}(r_{\lambda}^{\Delta'}) \text{Im } G_{\Delta\Delta'}^{\gamma}(r_{\lambda}^{\Delta}, \Omega_k^2) \quad (8)$$

where $G_{\Delta\Delta}^{\gamma\gamma'}(r_{\lambda}^{\Delta})$ is a Green function (γ and γ' are numbers of interacting coordination spheres) defined as:

$$G_{\Delta\Delta}^{\gamma\gamma'}(r_{\lambda}^{\Delta}) = \sum_{\varphi} \{ \langle \eta | V_{e-ph}(r_i) | \varphi \rangle \langle \varphi | \mathbf{d} | \xi \rangle + \langle \eta | \mathbf{d} | \varphi \rangle \langle \varphi | V_{e-ph}(r_i) | \xi \rangle \} (E_{\xi} - E_{\eta})^{-1} \quad (9)$$

The Green function calculations were carried out for a perfect BBO lattice renormalized by glass-like environment with taking into account effective nanocrystallite sizes and by performing the summations over 125 k-points in the irreducible part of the quasi-Brillouin zone. The resulting expression is given below:

$$G_{\Delta\Delta}^{\gamma\gamma'}(r_{\lambda}^{\Delta}, \Omega_k^2) = \sum_{\Omega} K_{\Delta}^{\gamma\gamma'}(r_{\lambda}^{\Delta}) K_{\Delta}^{\gamma\gamma'}(r_{\lambda}^{\Delta}) (\Omega_k^2 - \Omega^2 - i\delta)^{-1} \quad (10)$$

where the coordinates $K_{\Delta}^{\gamma\gamma'}(r_{\lambda}^{\Delta})$ were obtained for a given quasi-phonon type by means of the electron states averaging. The vacancy-induced lattice perturbation of the Green function has been done using a deformation localization that allows us to use a Dyson relation:

$$G_{\Delta\Delta}^{\gamma\gamma'}(1) = G_{\Delta\Delta}^{\gamma\gamma'}(0) + G_{\Delta\Delta}^{\gamma\gamma'}(0) U G_{\Delta\Delta}^{\gamma\gamma'}(1) \quad (11)$$

where $G_{\Delta\Delta}^{\gamma\gamma'}(0)$ and $G_{\Delta\Delta}^{\gamma\gamma'}(1)$ is the Green function for an ideal and vacancy-perturbed system, respectively. Coming out from the equation (11), we have obtained the effective electron-phonon wavefunctions for calculations of the intra-the-cluster electrostatic potential and corresponding phonon modes before and after applying the acoustical waves. Afterwards the interaction of the defects with appropriate phonon modes has been taken into account. The changes of effective electrostatic potential contours and of effective low-frequency vacancy modes under influence of external photoinducing field show that the applied photoinducing field essentially changes the electrostatic potential distribution. The appearance of additional non-centrosymmetry in the electrostatic potential distribution is a main requirement to enhance of the second-order nonlinear optical properties, particularly of the SHG, and such an effect is unambiguously seen in this case. Comparison of the calculations made before and after applying of photoinducing field indicates on essential charge density redistribution before illumination and after the illumination. The branches corresponding to the acentric symmetry are responsible for the SHG and the centrosymmetric ones for the TPA.

3. CONCLUSIONS

In conclusion it is necessary to underline that:

Experimentally and theoretically was revealed an occurrence of the non-centrosymmetry due to the disappearance of long-range ordering in the BiBO glass.

Increased non-crystallinity stimulates an enhanced SHG.

Two-photon absorption is critically dependent on the hydrostatic pressure.

Band energy structure calculations confirm essential redistribution of the valence electronic states during the photoinducing illumination.

REFERENCES

1. H. Hellwig, J. Liebertz, L. Bohaty, "Exceptional large nonlinear optical coefficients in the monoclinic bismuth borate BiB_3O_6 (BIBO)", *Solid State Comm.*, **109**, No.4, pp. 249-251, 1999.
2. D. Xue, S. Zhang, "Structural analysis of nonlinearities of $\text{Ca}_4\text{ReO}(\text{BO}_3)_3$ (Re= La, Nd, Sm, Gd, Er, Y)", *Applied Physics a - Mat. Science and Processing*, **68**, pp. 57-61, 1999.
3. Z.G. Hu, T. Higashiyama, M. Yoshimura, Y.K. Yap, Y. Mori, T. Sasaki, "A new nonlinear optical borate $\text{K}_2\text{Al}_2\text{B}_2\text{O}_7$ ", *Jpn. J. Appl. Phys.*, Vol. **37**, pp. L1093-1094, 1998.
4. Y. Mori, I. Kuroda, T. Sasaki, S. Nakai, "Nonlinear optical properties of cesium lithium borate", *Jpn. J. Appl. Phys.*, **34**, pp. L296-L298, 1995.
5. L.K. Cheng, W. Bosenberg, C.L. Tang, "Growth and characterization of low temperature phase barium metaborate crystals", *J. Cryst. Growth*, **89**, pp. 553-559, 1988.
6. J.D. Bierlein, and H. Vanherzeele, "Potassium titanyl phosphate: properties and new applications", *J. Opt. Soc. Am. B*, Vol. **6**, No. **4**, pp. 622-633, 1989.
7. J. Liebertz, "Crystal growth from melts of high viscosity", *Prog. Crystal Growth and Charact.*, **6**, pp. 361-369, 1983
8. I.V. Kityk, and B. Sahraoui, "Photo induced two-photon absorption, and second harmonic generation in As_2Te_3 - CaCl_2 - PbCl_2 glasses". *Physical Review(USA)*. V. **60**, No. **1**, pp. 942-949, 1999.